Power System Technology
ISSN:1000-3673

Received: 06-06-2024 Revised: 15-07-2024 Accepted: 28-08-2024

Presenting a New Method for Reconstructing and Revealing Metal Areas in Real Raw Data (Cyanogram Improved with Tooth Filling Materials) To Reduce the Effect of Various Distortions in Two-Dimensional Scan Images of Spiral-Shaped Metal Implants and Dental Prostheses Instead of Reconstruction Cuts. Done Using LBF And FBP Methods

[1]Bita Aramesh, [2]Artam Enayat, [3]Melika Espahbodi, [4]Akram Mona Ghannadpour, [5]Shahab Honar

[1]Specialist in surgery and root canal treatments (Endodontist), University of Sistan and Baluchistan, Zahedan, Iran
dr.aramesh20@yahoo.com
[2]Tehran University of Medical Sciences, Doctor of dental surgery (DDS)
artamenayat@gmail.com
[3]Tehran University of Medical Sciences, Doctor of dental surgery (DDS)
melika.esp@icloud.com
[4]Tehran University of Medical Sciences, Doctor of dental surgery (DDS)
ghannadpour.dds@gmail.com
[5]Shiraz University of Medical Sciences, Master of Periodontics in Dentistry (DDS, Ms.D)
shahab.honar.dds@gmail.com

Abstract

A growing demand for the use of tomography is now commonplace in the field of implantology, not only to guide diagnosis and treatment planning, but also to perform postoperative evaluations when clinical examination and conventional radiography do not provide adequate diagnosis. Is. Information. However, when implants are present, images are affected by high-density material. This creates so-called artifacts that interfere with image quality and lead to a questionable diagnostic value, which in turn may lead to misinterpretations. Considering the role of CT scan in the diagnosis of oral and dental diseases and the importance of improving the resulting images, efforts and studies to reduce the impact of various distortions, including distortions caused by the presence of metal tissues in the skull and mouth, have long been required. attention has been In this research, a new method for reconstructing images and detecting metal regions in raw data (improved cyanogram) was investigated in order to reduce the effect of various distortions in two-dimensional scan images of spiral-shaped metal implants and dental prostheses instead of sections reconstructed with the method. FBP has been paid. The algorithm that is considered

Power System Technology
ISSN:1000-3673
Received: 06-06-2024 Revised: 15-07-2024 Accepted: 28-08-2024

for comparison with the main algorithm proposed in this article is the use of a threshold limit instead of the FBP active contour model for initial separation; That means, first, by using a threshold limit, the metal regions in the sinogram image are separated with very low accuracy. Then by applying the mentioned Hough transformation to the separated parts, these areas are identified with high approximation. The result of applying this algorithm to the real data (sinogram image of the patient with tooth filling material and hip prosResearch) and the data related to the mentioned mollage scan sinogram along with the results of the main algorithm are obtained. Compared to the original algorithm, the results of this algorithm are the same for the data related to mollage and for the data related to the patient with dental filling materials and hip prosResearch of lower quality. In fact, because the dental filling materials are small and large, as well as the number of hip prosResearch parts for the relevant data in this research is high, and on the other hand, the data is related to the spiral CT scan.

Keyword: improved cyanogram detection, tooth filling, distortions, scan images, metal implants, dental prostheses

1. Introduction

Image artifacts are defined as any distortion observed in the reconstructed images and not related to the investigated object [1, 2]. Factors causing artifacts in CBCT images may be mainly related to high-density materials and some device parameters, such as FOV (field of view) size. Other parameters also change image quality, including kilovoltage (kV), milliamperes (mA), and voxel size (element volume). Other factors such as device calibration and patient movements can also produce artifacts [3]. Metal objects in patients can cause many physical effects such as noise, beam hardening, scattering and image starvation on image quality [4]. An implant can produce beam-hardening artifacts where white and black lines are shown [5], obscuring anatomical structures and affecting the contrast between adjacent regions. Therefore, these effects can seriously interfere with the detection process using images.[6]

In the meantime, it is necessary to know how to establish and function the body's organs in normal conditions and their changes due to illness in order to understand and justify the occurrence of signs and symptoms. Although anatomy or the knowledge of internal organs and systems through direct contact and cutting of the human body provides comprehensive information to doctors and medical scholars, it is limited to the exclusive use of this method to know the physical condition. And the function of the internal tissues is not only not always possible, but it can cause considerable damage to humans. Using previous experiences on corpses and generalizing individual findings is also not possible due to the significant differences in the anatomy of the human body. Therefore, the use of tools and

Power System Technology
ISSN:1000-3673
Received: 06-06-2024 Revised: 15-07-2024 Accepted: 28-08-2024

technology to obtain accurate information from the inside of humans has been one of the never-ending ideals of medical scholars. Throughout history, the idealism of medical scholars in obtaining more complete information from inside the human body has led them to create, develop and use technology[7]. After the invention of CT, image reconstruction with FBP method was introduced for physical applications. To date, FBP remains the most widely used image reconstruction method in CT. This method is called a so-called transformation method because it is based on the assumption that measurements, Radon transformation of linear attenuation coefficient distribution and analytical inverse of Radon transformation is a direct solution for image reconstruction. If this algorithm to ideal projections; That is, to apply an unlimited number of measurements with unlimited narrow beams and without noise, then this solution is ideal. But in practice it is not like this. Because first, the measurements are read with a limited number of detectors in a limited rotation interval and using limited wide beams. Secondly, the x-ray tube emits a continuous spectrum that is created as a result of the hardening of the rays [8]. Third, the measurements are noisy and include scattered radiation [9]. There are many other differences between the real measurements and the Radon transformation, all of which cause artifacts in the reconstructed images. But usually the errors caused by these approximations are relatively small and the FBP results are satisfactory. In addition, artifacts can be reduced by applying corrections before or after applying FBP. For example, noise and artifacts caused by aliasing are reduced by applying a low-pass filter to the raw data. However, under many events, including the presence of high-density objects, the artifacts become incredibly intense. [10] Many researchers have tried with different methods to eliminate metal artifacts, and they are usually based on the assumption that the measured information is affected by metal objects, or They are ignored or replaced through interpolation between neighboring sizes. These existing algorithms lead to a drastic reduction of metal artifacts, but some of them create new artifacts. Therefore, better algorithms are needed to reduce metal artifacts more effectively [11].

In CT topics, the most important causes of metal artifacts that appear as dark and light lines are: beam hardening, lack of photons, scattering and relative volume effect, which are mentioned in the following definition [2-3].

Figure 1: CT images of the skull that include dental filling materials [3].

Power System Technology
ISSN:1000-3673
Received: 06-06-2024 Revised: 15-07-2024 Accepted: 28-08-2024

In the image reconstruction process, it is assumed that monochromatic X-rays are used. But in practice, the X-rays that are used have a wide energy spectrum. Therefore, when a group of rays is irradiated to objects, those rays that have a higher attenuation coefficient; That is, they have a low energy spectrum and are removed from the radiation group sooner. Therefore, the average energy of the beam increases and its penetration ability increases. Generally, the types of rays whose energy spectrum is in the range that is more easily weakened are called soft X-rays, and those that penetrate more into objects are called hard X-rays. called Therefore, the phenomenon of hardening of rays can be seen as the disappearance of soft X-rays from a group of X-rays with a wide range of energy spectrum, the rest of which will be hard rays. The amount of hardening of the rays depends on the extent of their energy spectrum and the composition of the materials that pass through it. As a result, the rays passing through denser materials such as metals will make them harder. Therefore, the amount of attenuation of these rays decreases, and when they reach the receiver, they will be more intense than expected, which will appear as bright lines in the image [12].

When X-rays pass through metal areas, they will be greatly weakened and not enough photons will reach the receivers. The result will be creating an image with a lot of noise at certain angles. If at these angles, the current passing through the generating tube increases in order to increase the intensity of these rays, the problem of this distortion will be solved. But the disadvantage of this is that the patient receives too much X-ray in scanning other angles [13].

Many X-ray photons that penetrate an object are subjected to Compton scattering. In this type of scattering, a radiation photon with a relatively high energy hits a free electron from the outer layer of the atom and takes it out of its orbit. The said photon is deflected and moves in a new direction as a scattered ray. Almost all scatterings come from this collision. The probability of a Compton collision is influenced by the energy of the beam and the density of the absorbing material. It is obvious that these photons are useless for image reconstruction and care should be taken not to use them in reconstruction.

The distortion caused by this effect occurs when a high-density object is incompletely placed in a section and the rest of it is not located in that section. As a result, when this object is placed in the path of the ray, its density is displayed lower than the real limit. If only one object is partially placed in the section, the measurement error is the same in all sections, but if two or more objects with high density are partially placed, then the measurement error is non-linear and in the form of radii. that pass through these objects are displayed in the image. This non-uniform information creates a linear artifact [14].

In this article, a new method for reducing metallic artifacts in spiral CT scan images that uses a fan-shaped beam is described. The basis of this method is the separation of metal

Power System Technology
ISSN:1000-3673
Received: 06-06-2024 Revised: 15-07-2024 Accepted: 28-08-2024

regions in raw data (sinogram) instead of reconstructed slices, with active contour and two-dimensional Hough transform methods. In this way, among the latest active contour methods, the best model called LBF is used to find the approximate borders of the areas with metal artifacts. After that, a method based on the Hough transform, which is designed based on the sinogram equation of fanning rays, is applied to the sinogram image to find all the sinusoidal curves that are related to the metal artifact. Finally, all the found pixels are black and then their intensity is replaced based on the intensity in the artifact-free projections obtained at the opposite angle. In fact, this method has been considered and tested for patients who have metal objects, such as prostheses or dental filling materials. [15] Considering the role of CT scan in the diagnosis of diseases and the importance of improving the resulting images, efforts and studies to reduce the impact of various distortions, including distortions caused by the presence of metallic tissues in the body, have long been considered. have been. In this chapter, a brief review of various opinions in this field is discussed. [16]

The most basic and simplest proposal to reduce metal artifacts was proposed by Ibrahim in 1990, who instead of using metal prostheses in orthopedics used another kind [11]. But this proposal is not suitable for cases where the distortion is caused by an object other than a prosResearch (for example, a metal artificial tooth or the presence of a bullet in the body).

Mr. Manken points out in a theory in 2003 that it can be reconstructed by using the weighted sum of sinogram values in the neighboring points of a desired point [13]. Neighborhood points, by definition, is a window centered on the desired point. It has also been stated that the coefficients of this weighted sum are only a function of the distance of each point from the center of the window. Although in this method, more healthy points participate in the reconstruction of each point, but the implementation of this method does not maintain the continuity of the structure of the reconstructed points and therefore increases the risk of increasing noise. Meanwhile, in his activity, Dr. Yazdi presents an algorithm for interpolation and reconstruction of lost points, by which the structure of points close to the reconstructed points is preserved. In this algorithm, the goal is that the interpolation is done between two areas that are related to the same texture instead of between two points located in the same column.

In 2005, Dr. Yazdi and colleagues designed a three-step method to reduce metal artifacts caused by hip prosResearch [16]. This method includes an automatic algorithm for metal implant detection, a modification algorithm for projections and a new and optimal algorithm for interpolation. Finally, the enhanced raw data is transferred to the scanner to create the enhanced image. In 2006, Dr. Yazdi and colleagues proposed a method to remove distortions in CT scan images [17]. In this design, first, the areas related to metal textures are determined

Power System Technology
ISSN:1000-3673
Received: 06-06-2024 Revised: 15-07-2024 Accepted: 28-08-2024

in the sinogram matrix. For this purpose, first, an initial image is formed using a full circle (360 degrees) of the sinogram matrix based on figure "2-b". Since metallic textures create continuous points with high intensity values in the image, a threshold limit is defined by using a fraction of the maximum value in this image so that the areas can be specified related to the metal texture according to figure "2-c". Then, the exposed metallic textures are again converted into a sinogram image using the FBP algorithm according to Figure 2-d, so that the approximate range of these textures can be determined in the original sinogram matrix. After identifying the areas related to the metal texture in the sinogram, these areas are reconstructed with artifact-free points in the slice with the opposite angle according to figure "2-f".

In 2009, Hui Xue et al proposed a method to reduce metal artifacts in dual-energy CTs based on active contour methods [18]. In this method, assuming that the sinogram consists of two regions, one of metallic texture and the other of non-metallic texture, with continuous intensity in the regions, the geometric active contour method proposed in [19] is used to separate the boundary of metallic regions. to be After separating and setting the intensity of the found areas to zero, the sinogram is improved with the point interpolation algorithm called TV painting and the final image is formed from it. Among the disadvantages of this method is that the mentioned active contour is not suitable for sinograms that have heterogeneous intensity, and on the other hand, the separation accuracy with only the active contour method is low.

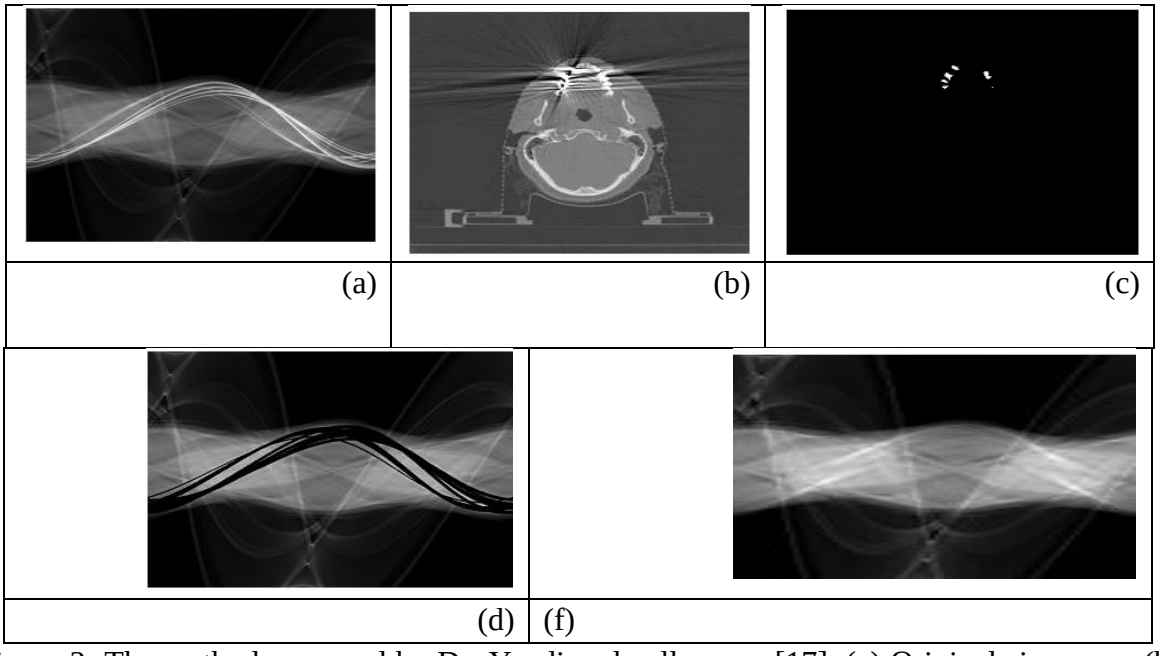

Figure 2: The method proposed by Dr. Yazdi and colleagues [17]. (a) Original sinogram. (b) Original CT image. (c) Detection of metallic objects. (d) Converting metallic textures to sinogram. (f) recovery of sinogram points (d) with the proposed method

Power System Technology
ISSN:1000-3673
Received: 06-06-2024 Revised: 15-07-2024 Accepted: 28-08-2024

In 2020, Vetter et al focused on accurate and optimal separation of metal regions only in the sinogram image to reduce the metal artifact [20]. They believed that direct separation in the sinogram image is optimal and different from other separation methods on reconstructed images with Radon transformation. This method is based on the use of Bayesian techniques and Markov random model. After separating the metal regions, the interpolation method is used to restore and improve the sinogram.

By examining the mentioned activities, it can be said that the general process of the methods is the same. In this way, first, using different methods, the direct or indirect separation of metal textures in the raw data image is addressed. Then, using different interpolation algorithms, the found areas are replaced with new values to improve image quality.

2- Research method

The most optimal methods to reduce the artifact are performed on sinogram images. In most of the publications based on this topic, revealing the projection information in the sinogram space that has been affected by metal objects is based on separating the metal objects in the CT images and returning the image of only the metal to the sinogram image [17, 21]. . Direct separation and correction in the original sinogram image eliminates the need for complex calculations to transform the reconstructed image into a sinogram [20, 18]. In addition, such a method can correct metal artifacts that originate from prostheses outside the field of view. For this reason, the proposed method in this research is presented on this basis.

On the other hand, it has been suggested for the cases where the metal tissues are bulky and their number is small, and in cases where these tissues are small and many, such as tooth fillings, they do not show their ability well. give For this reason, in this research, such metal textures are investigated.

Considering that the proposed algorithm is applied to the medical data obtained from the spiral CT scan, at the beginning, a brief discussion about the spiral CT scan and sinogram formation is given, and finally, the proposed algorithm is presented.

2-1- The proposed algorithm

In the proposed algorithm, having raw data, sinogram image formation is done first. In case of observing scattered points with very high frequency, if necessary, by applying low-pass filters to the image, very high frequencies can be reduced for better separation of metallic textures in the sinogram. After that, one of the best active contour models is applied to the image to determine the boundaries of the areas affected by the metallic textures. Finally, a method based on two-dimensional Hough transform and then an algorithm for post-processing is applied to more accurately separate the mentioned areas into designated areas.

Power System Technology
ISSN:1000-3673
Received: 06-06-2024 Revised: 15-07-2024 Accepted: 28-08-2024

It is the chosen model in this research and for this reason it is described more fully. Like the second model, this model was proposed by Lee et al. and it is generally referred to as the local binary matching model, and like the previous models, it is based on curve evolution methods, Mumford-Shah function [22] and level set [23] is

Considering I as the gray level image, Ω as the defining dimension of the image and C the closed contour that moves in the image dimension and divides it into two parts 〖Ω〗_1 and 〖Ω〗_2, for each point The energy function XϵΩ is defined by relation (1):

$$\varepsilon_X\big(C, f_1(X), f_2(X)\big) = \sum_{i=1}^{2} \lambda_i \int_{\Omega_i} K(X-y)|I(y) - f_i(X)|^2 \, dy \qquad (1)$$

$$\frac{\partial \emptyset}{\partial t} = -\delta_\varepsilon(\phi)(\lambda_1 e_1 - \lambda_2 e_2) + \upsilon\delta_\varepsilon(\phi)\mathrm{div}\left(\frac{\nabla\phi}{|\nabla\phi|}\right) + \mu(\nabla^2\phi - \mathrm{div}(\frac{\nabla\phi}{|\nabla\phi|})) \qquad (2)$$

where λ_1 and λ_2 are constant positive values and equal to one for this project. f_1 (X) and f_2 (X) estimate the image intensity values in 〖Ω 〗_1 and 〖Ω 〗_2, respectively. It can be shown that these functions are the weighted average of the intensity of images in a neighborhood of point X. The intensities of I(y) in a region centered on point X are selected, and the size of the radius of this region is controlled by the kernel function K. The choice of this kernel function is free, but it must meet the following conditions:

- $K(u) = K(-u);$
- $K(u) \geq K(v), \text{if } |u| \leq |v| \text{ and } \lim_{n\to\infty} K(u) = 0;$
- $\int K(u)du = 1;$

In this research, the Gaussian function with a standard deviation of 3 is used. Then the defined energy function is reconstructed as level set formula. Finally, by minimizing the energy function with respect to the level set function ϕ and considering C as the zero level set, the curve evolution equation is obtained as relation (2):

$$\frac{\partial \emptyset}{\partial t} = -\delta_\varepsilon(\phi)(\lambda_1 e_1 - \lambda_2 e_2) + \upsilon\delta_\varepsilon(\phi)\mathrm{div}\left(\frac{\nabla\phi}{|\nabla\phi|}\right) + \mu(\nabla^2\phi - \mathrm{div}(\frac{\nabla\phi}{|\nabla\phi|})) \qquad (2)$$

where δ_ε Dirac's delta function is defined as relation (3) and also e_1 and e_2 according to relation (4-4). In this research, the constant values of υ and μ are chosen as 1.001×255×255 and 1, respectively.

Power System Technology
ISSN:1000-3673
Received: 06-06-2024 Revised: 15-07-2024 Accepted: 28-08-2024

$$\delta_\varepsilon(x) = \frac{1}{\pi}\frac{\varepsilon^2}{\varepsilon^2+x^2} \quad (3)$$

$$e_i(x) = \int_{\Omega_i} K_\sigma(y-x)|I(x) - f_i(y)|^2\, dy \quad (4)$$

It should be mentioned that the size of the kernel function K can be changed using the controllable parameter σ. The result of applying this model on the sinogram image can be seen in Figure 3-a and c. As it can be seen, the reason for the superiority and choice of this method compared to the second model is the less undesirable areas caused by separation.

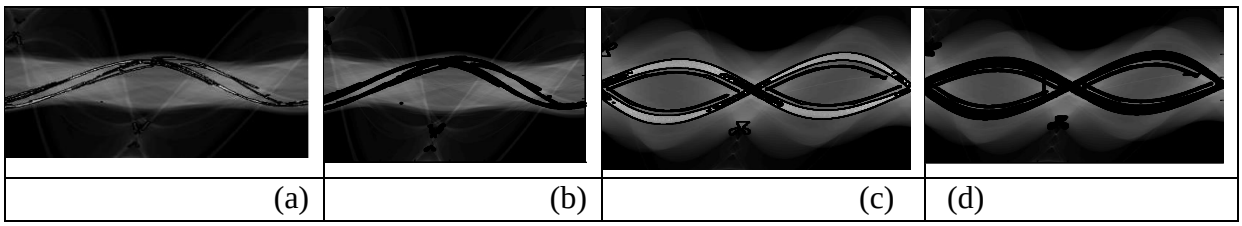

(a) (b) (c) (d)

Figure 3: Separation of metallic textures in sinogram with active contour model in [24]. (A) and (C), respectively, related to the patient with dental filling material and the patient with prosResearch, which separation is marked by black contour. (b) and (d) filling of the detected areas as black dots

2-2- Algorithm based on Hough transform

After the approximate separation of the areas related to the metal texture in the sinogram using the LBF model, in order to separate these areas more precisely, an algorithm based on the two-dimensional Hough transform is proposed in this research.

Hough transform can be generalized to any function. In such a way that the said algorithm is based on the sinogram equation for fan beams. In other words, the purpose of designing this algorithm is to find all the sinusoidal curves related to the metal texture in the sinogram space using the voting method. This voting method is performed in a parameter space where the candidates related to metal textures are obtained as a local maximum in the accumulator space. In the implementation of this method, the data of all the areas determined by the LBF method are used according to Figure "3-b". Two-dimensional Hough transformation is used to find r_x and β_x parameters. The parametric space or two-dimensional accumulator space with dimensions r_x and β_x is made according to equation (5). As it can be seen in relation (5), every random point in the found area defined by (r_x, β_x) is mapped as a curve in the accumulator space.

$$r_x = \frac{Rtg(\gamma)}{\sin(\beta-\beta_x) + tg(\gamma)\cos(\beta-\beta_x)} \quad (5)$$

Power System Technology
ISSN:1000-3673
Received: 06-06-2024 Revised: 15-07-2024 Accepted: 28-08-2024

that the ranges determined for r_x and β_x are as $0 \leq r_x \leq r_{x,max}$ $0 \leq \beta_x \leq 2\pi$, where $r_{x,max}$) is based on the maximum field of view in CT system It is determined in practice. The steps of this algorithm can be described as follows:

Constructing a two-dimensional accumulator space for parameter space (r_x, β_x) and initializing all accumulator elements to zero.

Perform steps 3 to 8 for each point of the specified area.

Perform steps 4 to 5 by increasing β_x from 0 to π 2.

Obtain($r_x$using the formula (5).

If the obtained ($r_x$is within the specified range, then the array corresponding to that value is increased by one unit in the accumulator.

Perform all the above steps for all the points of the areas found in the sinogram.

Checking the accumulator to find the highest local vote for (r_x, β_x) related to the metal texture curve in the sinogram.

After selecting the candidates from the accumulator space, the curve corresponding to each candidate (r_x, β_x) is drawn in the sinogram space and then to prepare the sinogram for the interpolation operation, the pixels corresponding to each curve in the sinogram are blacked out.

Since in spiral imaging, the information is continuous, therefore, each part of the sinogram can be considered as a 360-degree cycle and image reconstruction can be performed at that point. This great advantage of spiral CT scan enables doctors to take pictures of any part of the body that is needed. In spite of this, this is not possible in normal CT scans, and as a result, no information is obtained from significant parts of the patient's body. The purpose of stating this is to remind that if for any reason, for example, the presence of metal tissue in the body, it is necessary to improve the quality of the image, it is better to apply quality improvement algorithms on the sinogram. Because if in the spiral CT scan, the quality improvement algorithm is performed on the final image, it practically deprives the doctor of the possibility that the spiral CT scan gives to the doctor by collecting continuous information, and if the quality of a CT image is improved If, for some reason, the doctor finds the need to create a cross-sectional image different from the previously taken image, the image improvement operation must also be implemented on the new image. Meanwhile, if the quality improvement algorithm is performed on the primary data of the sinogram, this quality improvement does not need to be repeated, it does not destroy the characteristic of the

Power System Technology
ISSN:1000-3673
Received: 06-06-2024 Revised: 15-07-2024 Accepted: 28-08-2024

spiral CT scan, and the doctor is able to reconstruct It creates more images at any desired time and of course with better quality and without the need to apply algorithms. For this reason, researchers in this field have directed their opinion more in this direction and perform their activities on sinogram.

Taking into consideration the mentioned materials, it was decided to apply the algorithms proposed in this research on the sinogram in order to use its advantages.

When the patient enters the cylindrical chamber of the device, the x-ray generator tube starts emitting radiation. These rays pass through the patient's body and reach the receptors located on the opposite side of the cylinder after different attenuations. Since the irradiated rays are fan-shaped or divergent in the CT scan machine, the generating tube irradiates the patient by creating a divergent beam from the X-rays. give The thickness of this beam is from 1 to 10 mm. Simultaneously with the uniform movement of the patient by means of a bed that is equipped with a motor, this x-ray generator tube rotates around the patient's body along with the receivers in front of it, and the number of rotations around the patient's body is It is chosen according to the case, so that this number of rotations changes from 10 to 50 numbers. It is obvious that the higher the number of these rotations for a specific shooting range, the higher the accuracy of the captured images and more details of the body will be examined.

According to figure "4", the angle of the ray generator is less than 180 degrees. Obviously, due to the distance between the patient and the radiation tube, this angle does not need to be large. Because due to the divergence of this beam, at a greater distance from the radiation tube, this beam covers a wider range. This productive viewing angle, which can be different in different devices made by manufacturing companies, is considered to be one of the characteristics of the device and is used as a known parameter in imaging operations. It should be noted that in the device examined in this Research, the viewing angle of the ray generator is 55 degrees.

As the generator and receivers start to rotate at every moment, the receivers record the intensity of the rays coming out of the patient's body and transfer them to the computer. In the next moment, these actions are repeated and the generator and receivers rotate one step in the same direction, and this action covers 360 degrees; That is, a complete round is repeated. During this period of full rotation, the patient also moves forward at a constant speed. After collecting the radiation intensity by the receivers and sending this information to the computer, a matrix of data is formed, each member of which represents the intensity of the radiation received at each stage and related to a receiver. It is special. According to the said content, it is possible to understand the size of each formed matrix after collecting data in each complete round. In fact, the stages of a full 360-degree rotation are equal to the number of columns of the data matrix. Also, the number of lines is equal to the number of receivers in

Power System Technology
ISSN:1000-3673
Received: 06-06-2024 Revised: 15-07-2024 Accepted: 28-08-2024

the CT scan machine, which record information at each step and each of them transmits their respective information to the computer. Therefore, in each complete round, information is collected in an mxn matrix, where m is the number of device receivers and n is the number of step rotations in a complete round. Due to the continuity of information in spiral CT scanning, it is not necessary to form a data matrix after each complete round and transfer it to the computer, but the information can be completely stored from the beginning of the scan to the end of it. continuously transferred to the computer and formed a sinogram with the number of lines equal to the number of receivers and columns equal to the total number of scanning steps. Then, to form the final image, he separated the required number of columns from this sinogram, formed a smaller matrix with the same number of rows, and finally performed the imaging operation on it. In other words, the selection of columns from the sinogram can be done in any way and the only limitation is the number of columns, which must be equal to n; That is, the number of rotations in a period of 360 degrees.

In the proposed algorithm, having raw data, sinogram image formation is done first. In case of observing scattered points with very high frequency, if necessary, by applying low-pass filters to the image, very high frequencies can be reduced for better separation of metallic textures in the sinogram. After that, one of the best active contour models is applied to the image to determine the boundaries of the areas affected by the metallic textures. Finally, a method based on two-dimensional Hough transform and then an algorithm for post-processing is applied to more accurately separate the mentioned areas into designated areas.

The proposed algorithm is based on the approximate separation of metal regions in the sinogram image with the active contour method and the application of the Hough transform method and the post-processing algorithm for more accurate separation. As can be seen in Figure 4, the result of this algorithm has been used to accurately separate these areas. In order to see better results from the design of this algorithm, the interpolation of the black points is done based on the method in [17] to judge the proposed algorithm based on the quality of the obtained image.

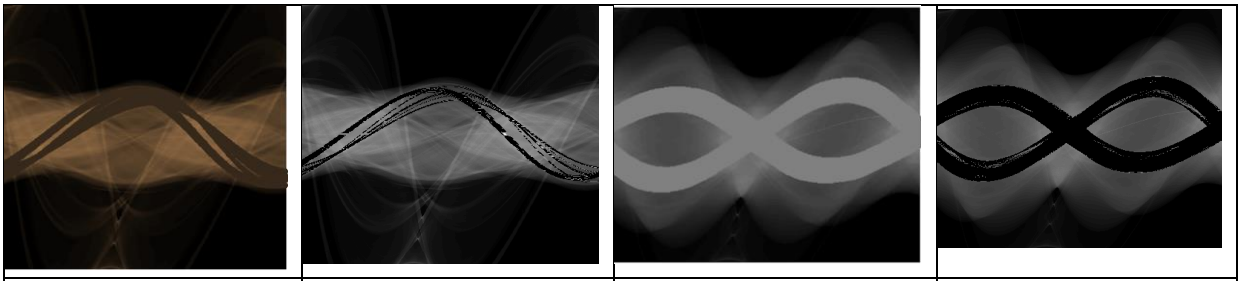

(a) (b) (c) (d)

Figure 4- Designed Hough transform applications (a) and (c) revealing all sinusoidal curves in the sinogram of patients with tooth filling materials and prostheses through the algorithm

Power System Technology
ISSN:1000-3673
Received: 06-06-2024 Revised: 15-07-2024 Accepted: 28-08-2024

based on Hough transform. (b) and (d) blackening the pixels corresponding to the curves revealed in parts (l) and (c).

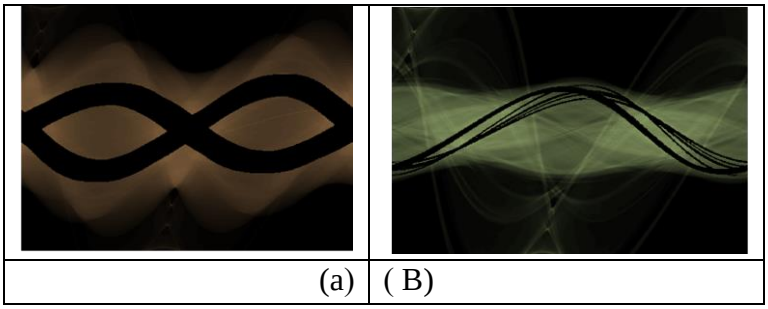

(a) (B)

Figure 5- Applying the method after processing. The result of the application on the images of "4-b and d" forms (a) and (b), respectively.

3-Results

In order to see the results of the proposed algorithm, this algorithm has been implemented in the MATLAB programming environment. It should be mentioned that this algorithm has been applied on the real data of patients, one patient with hip prosResearch and the other patient with tooth filling materials. In fact, each step of the desired algorithm is tested separately on the data to reveal the value of the existence of all steps. That is, first after separating the metal areas in the original sinogram images of patients with hip prosResearch and metal tooth filling materials; That is, figures "6-a" respectively by the LBF active contour method and the post-processing method, the isolated areas, according to figure "6-c" black and then respectively by the interpolation method in [6] and [17], it is reconstructed based on figure "3-d".

Considering a 360-degree cycle of the improved sinogram, the image reconstruction operation is performed at that point with the FBP method. As shown in Figure 3-H, the cross-sectional area of the jaw that includes tooth filling materials and Figure 7-F, the cross-sectional area of the pelvis that includes the prosResearch can be seen in these images compared to Reconstructed images of the same sections in the original sinogram, which includes the metallic stripe artifact. The result of applying this algorithm can be seen in figure "8-b" and "10-b". As can be seen in figure "8-c" and "9-c", all the metal areas in the sinogram have been improved in an excellent way, which is the result of the precise separation of the proposed algorithm. In order to observe other results of the optimality of this algorithm, different 360-degree cycles of the improved sinogram are selected and then the image reconstruction operation [17-6] is performed in those sections. The results of reconstruction of images from the improved sinogram along with the results of reconstruction of images from the original sinogram are shown in figures "9" to compare with each other.

Power System Technology
ISSN:1000-3673
Received: 06-06-2024 Revised: 15-07-2024 Accepted: 28-08-2024

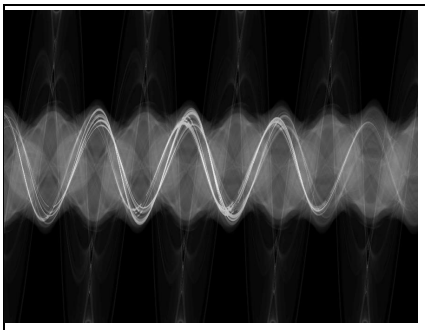	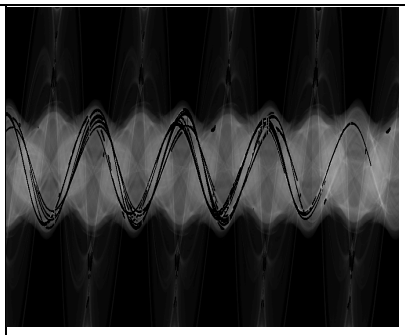	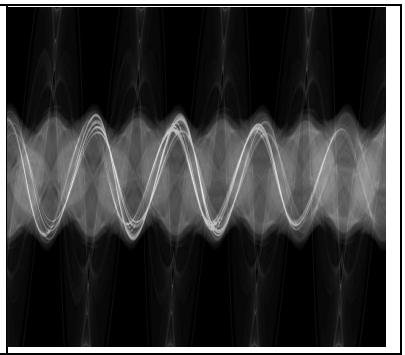
(c): reconstruction of black areas with the proposed method	(b): Blackening the isolated areas with the LBF method to prepare for interpolation	(A): Images of the main sinograms affected by the metallic texture.
	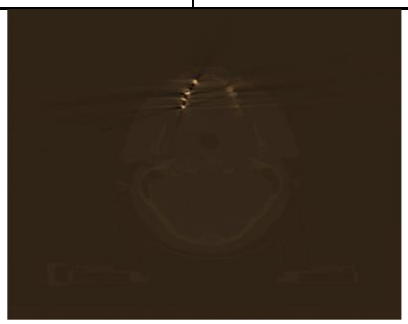	
H. Reconstruction of the image from the same section mentioned in (a) from the improved sinogram image of Figure 3-c.	d. Image reconstruction from a 360-degree cycle of the original sinogram image in Figure 3-A	

Figure 6- Applying the LBF method to the sinogram data and reconstructing the images from the improved sinogram after separation with only the LBF method.

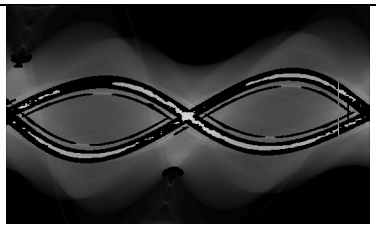	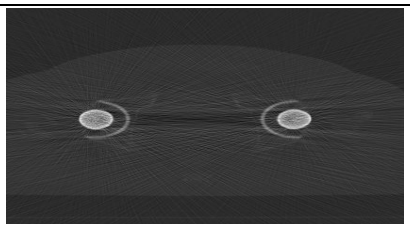	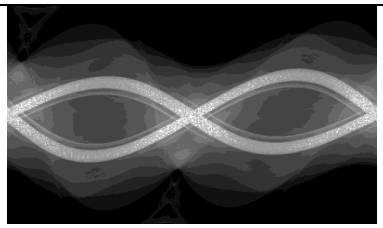
(c) blackening of the areas found by the LBF method and post-processing applied to it.	(b) reconstructed image from the sinogram (a) with metallic artifacts	(a) A 360-degree cycle of continuous sinogram that includes metal regions.

Power System Technology
ISSN:1000-3673
Received: 06-06-2024 Revised: 15-07-2024 Accepted: 28-08-2024

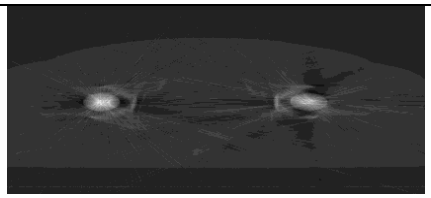

(f) Image reconstruction from the enhanced sinogram in (d).

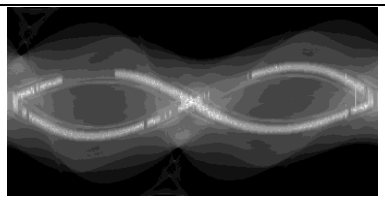

(d) Interpolation of black points in (c) with the method proposed in [15].

Figure 7: Applying the algorithm on a sinogram with metal areas caused by the presence of a prosResearch in the patient.

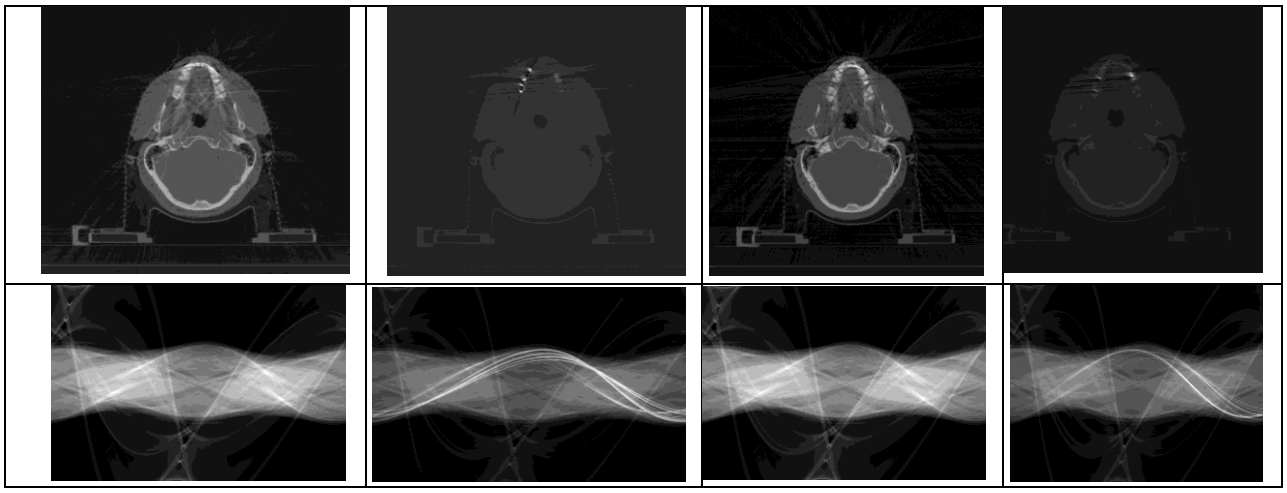

Figure 8: The results of reconstruction of images from the improved sinogram with the proposed method, along with the results of reconstruction of images from the original sinogram of the patient with tooth filling materials. Left column: Sinogram images of the patient with improved tooth filling materials are shown at the bottom of each original sinogram. Right column: reconstructed images from sinogram in front of them

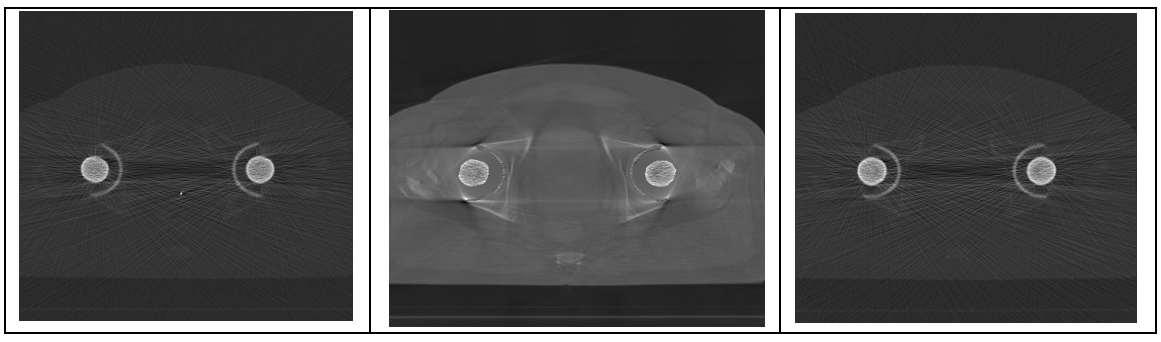

Power System Technology
ISSN:1000-3673
Received: 06-06-2024 Revised: 15-07-2024 Accepted: 28-08-2024

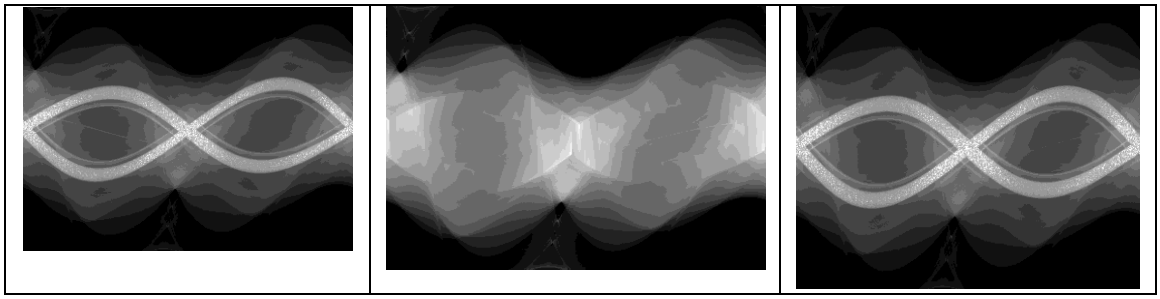

Figure 9: The results of reconstruction of images from the improved sinogram with the proposed method, together with the results of reconstruction of images from the original sinogram of the patient with hip prosResearch. Left column: sinogram images related to the patient with hip prosResearch, whose improvements are shown at the bottom of each main sinogram. Right column: reconstructed images from sinogram in front of them.

In order to better evaluate the performance of the proposed method with quantitative criteria and the possibility of comparing it with the image without distortion related to each slice, the algorithms presented in this research have also been implemented on a skull montage in Figure 10-A. . For this purpose, first, this montage was scanned by a CT scan machine made by Siemens company in the Hotel Dive Hospital in Quebec City, Canada, by Mr. Yazdi and his colleagues. The images obtained from this scan were considered as undistorted images. After that, some metal pieces that were a model of tooth filling were placed inside this mollage according to figure "10-c" and this mollage was scanned again. The resulting images were also saved as distorted images. After applying the proposed algorithms in this Research, images are obtained which are also named as improved images. Finally, a comparison is made between healthy images, distorted images, and improved images with different criteria, including the mean and variance of the gray level, the mean square of errors, the maximum signal-to-noise ratio, and the Q parameter, which are explained below. They will be. It should be mentioned that moulage in different states, that is; It has been scanned with metal parts in different positions and numbers inside it, and in this research, in each scanning mode of the mollage, one or two slices have been proposed, selected and tested for applying the algorithm. The result of these images along with their corresponding sinograms in three modes of mollage without metal, mollage with metal and the image created from the improved sinogram, in "11" forms, as well as the results of comparing these images with the introduction criteria. It is shown in "5" tables.

Power System Technology
ISSN:1000-3673
Received: 06-06-2024 Revised: 15-07-2024 Accepted: 28-08-2024

(a) (b) (c)

Fig. 10- Mollage of the skull. (a) Mollage without metal objects. (b) teeth and metal materials to be placed in the mollage. (c) Mollage with teeth and metal materials.

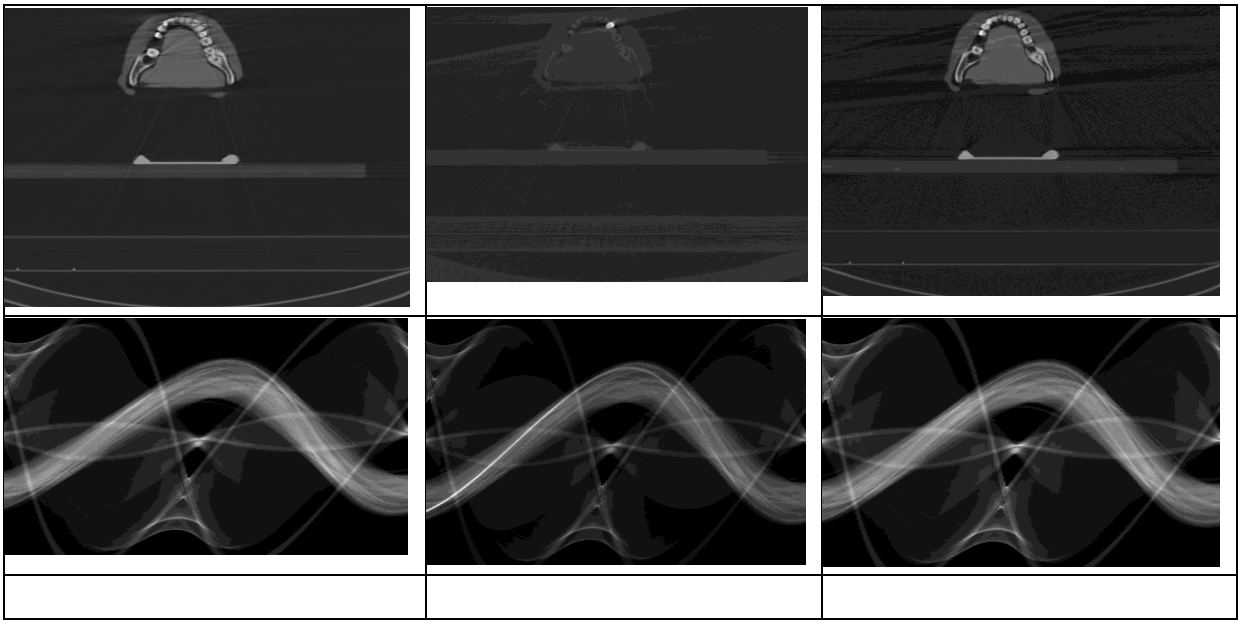

Figure 11- The results of reconstruction of images from sinogram improved with the proposed method, together with the results of reconstruction of images from sinogram related to mollage with and without metals. The left column from the top, middle and bottom, respectively, shows the sinogram images related to the moulage without metal, moulage with metal and improved. Right column: reconstructed images from sinogram in front of them.

Table 1: Comparison of images without distortion, with distortion and improved Figure 11.

Q	PSNR	MSE	Gray level average	gray level variance	
			178.858	84.56868	Image without

Power System Technology
ISSN:1000-3673
Received: 06-06-2024 Revised: 15-07-2024 Accepted: 28-08-2024

					distortion
0.45673	17.3447	916.1634	15.896	58.589	Distorted image
0.44582	32.946	52.7906	202. 8785	91.6789	Improved image

The algorithm that is considered for comparison with the main algorithm proposed in this research is the use of a threshold limit instead of the active contour model for initial separation; That means, first, by using a threshold limit, the metal regions in the sinogram image are separated with very low accuracy. Then by applying the mentioned Hough transformation to the separated parts, these areas are identified with a high approximation. The result of applying this algorithm to the real data (sinogram image of the patient with dental filling materials and hip prosResearch) and the data related to the sinogram of the mollage scan, together with the results of the main algorithm, are shown in Figure "12" it has been shown. As it can be seen, the results of this algorithm compared to the original algorithm are the same for the data related to the mollage and for the data related to the patient with dental filling materials and hip prosResearch of lower quality. . In fact, due to the fact that the dental filling materials are small and large, as well as the number of parts of the hip prosResearch for the relevant data in this research is high, and on the other hand, the data related to the spiral CT scan is identified and The separation of metal related areas is done with the threshold limit method with very low accuracy compared to the active contour model. Because in the threshold limit method, a general separation is performed and in the active contour method, a local separation is performed. However, the metal textures in the mentioned mollage are small and small, and for this reason, they are easily identified by the threshold method.

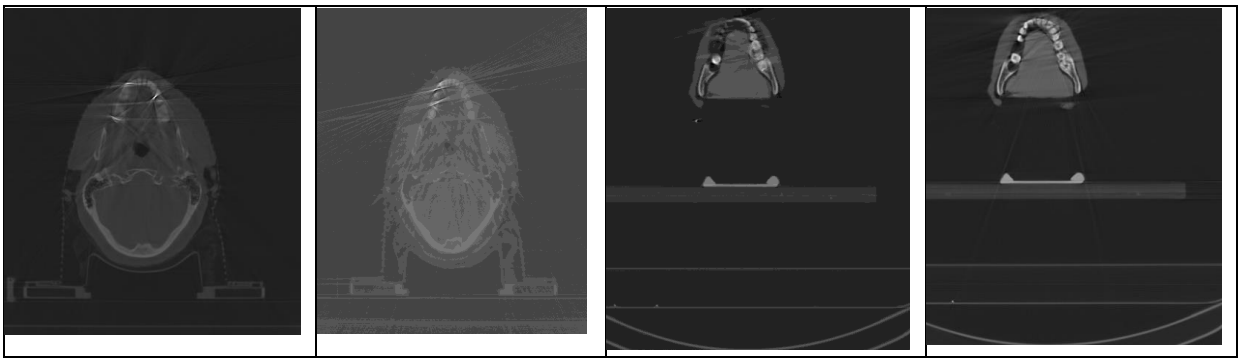

Power System Technology
ISSN:1000-3673
Received: 06-06-2024 Revised: 15-07-2024 Accepted: 28-08-2024

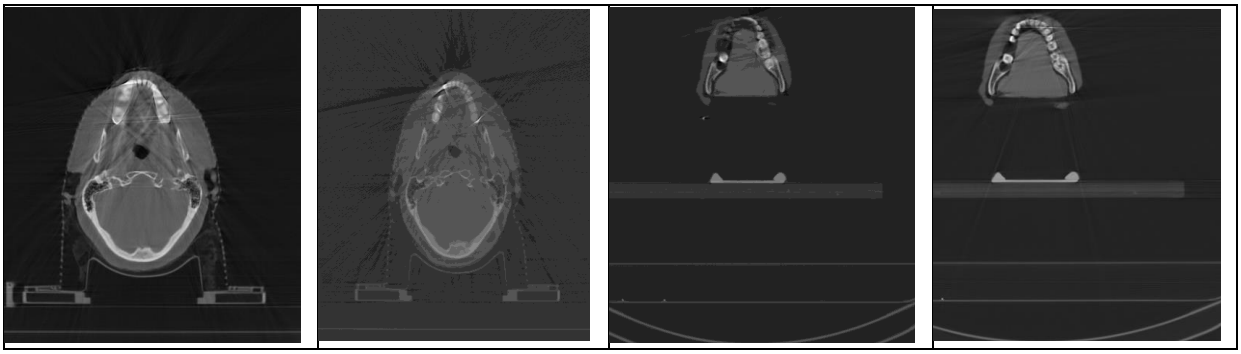

Figure 12: Comparison of the main algorithm with the separation method with threshold limit and Hough transform. Right column: image reconstruction results from improved sinogram with thresholded separation algorithm and Hough transform. Left column: image reconstruction results of improved cyanoxam with segmentation algorithm with active contour model and Hough transform

4- Conclusion

In addition to objectively observing the improvement in the quality of distorted images, it is carefully observed in Tables (1) that by applying the proposed method, the quality of the improved image has increased. Considering that the average and variance parameters of the gray level of the pixels have been calculated in the area related to the language texture and the language texture is more uniform compared to other areas, it can be seen that by applying the proposed algorithm done, the mean and variance of the gray level in this range has changed so much that it is closer to the mean and variance of the healthy image. Similarly, MSE and PSNR have decreased and increased significantly. Also, by observing the results of the Q parameter, it can be seen that these values have increased by approximately 0.1 or more for the improved images compared to the distorted images. [-1:1], is considered a very good increase. Also, the comparison of the threshold limit algorithm and Hough transform with the main algorithm shows the superiority of the active contour model over the threshold limit method.

References

1. Yazdi, M., and Beaulieul, L. (2007). "Artifacts in Spiral X-ray CT Scanners: Problems and Solutions," Proceeding of World Academy of Science, Engineering and Technology 26: 376-380.
2. Wang G, Snyder DL, O'Sullivan JA, et al. Iterative deblurring for CT metal artifact reduction. IEEE Transactions in Med. Imaging,1996; 15(5): 657-664.
3. de-Azevedo-Vaz S. L., Peyneau P. D., Ramirez-Sotelo L. R., de Faria Vasconcelos K., Campos P. S., Haiter-Neto F. Efficacy of a cone beam computed tomography metal artifact reduction algorithm for the detection of peri-implant fenestrations and

Power System Technology
ISSN:1000-3673
Received: 06-06-2024 Revised: 15-07-2024 Accepted: 28-08-2024

dehiscences. Oral Surgery, Oral Medicine, Oral Pathology, Oral Radiology . 2016;121(5):550–556.

4. Queiroz P. M., Santaella G. M., da Paz T. D., Freitas D. Q. Evaluation of a metal artefact reduction tool on different positions of a metal object in the FOV. Dento Maxillo Facial Radiology . 2017;46(3, article 20160366) doi: 10.1259/dmfr.20160366
5. Robertson DD, Yuan J, Wang G, et al. Total hip prosResearch metal-artifact suppression using iterative deblurring reconstruction. Journal of Comput. Assist. Tomogr., 1997; 21(2): 293-298.
6. Yazdi, M., and Beaulieu, L. (2006). “A novel approach for reducing metal artifacts due to metallic dental implants,” IEEE Nuclear Science Symposium Conference Record, vol. 4, pp. 2260–2263
7. Montesinos G. A., de Castro Lopes S. L. P., Trivino T., et al. Subjective analysis of the application of enhancement filters on magnetic resonance imaging of the temporomandibular joint. Oral Surgery, Oral Medicine, Oral Pathology, Oral Radiology . 2019;127(6):552–559. doi: 10.1016/j.oooo.2018.11.015Gregoris Rabelo L. E., Bueno M. D. R., Costa M., et al. Blooming artifact
8. Estrela C., Costa M. V. C., Bueno M. R., et al. Potential of a new cone-beam CT software for blooming artifact reduction. Brazilian Dental Journal . 2020;31(6):582–588. doi: 10.1590/0103644020200589 9Fontenele
9. R. C., Farias Gomes A., Rosado L. P. L., Neves F. S., Freitas D. Q. Mapping the expression of beam hardening artefacts produced by metal posts positioned in different regions of the dental arch. Clinical Oral Investigations . 2021;25(2):571–579.
10. Srinivasa N, Ramakrishnan KR, Rajgopal K. Image reconstruction from incomplete projection. Journal of Med. and Life Scienc. Eng., 1997; 14: 1-19.
11. Lewitt RM, Bates RHT. Image reconstruction from projections: III: projection completion methods. Optik, 1978; 50(3): 189-204.
12. Zhao S, Robertson DD, Wang G, et al. X-ray CT metal artifact reduction using wavelets: an application for imaging total hip prostheses. IEEE Transactions on Medical Imaging, 2000; 19(12): 1238-1247.
13. Mahnken, A.H., Raupach, R., and Wildberger, J.E. (2003). "A New Algorithm for Metal Artifact Reduction in Computed Tomograghy: In Vitro and in Vivo Evaluation after Total Hip Replacement," Invest Radiol, vol. 38, pp. 769-775.
14. reduction using different cone-beam computed tomography software to analyze endodontically treated teeth with intracanal posts. Computers in Biology and Medicine . 2021;136, article 104679 doi: 10.1016/j.compbiomed.2021.104679
15. Zhao S, Bae K.T, Whiting B, Wang G. A wavelet method for metal artifact reduction with multiple metallic objects in the field of view. Jourl. of X-Ray Science and Tech., 2002; 10: 67-76.

Power System Technology
ISSN:1000-3673
Received: 06-06-2024 Revised: 15-07-2024 Accepted: 28-08-2024

16. de-Azevedo-Vaz S. L., Peyneau P. D., Ramirez-Sotelo L. R., de Faria Vasconcelos K., Campos P. S., Haiter-Neto F. Efficacy of a cone beam computed tomography metal artifact reduction algorithm for the detection of peri-implant fenestrations and dehiscences. Oral Surgery, Oral Medicine, Oral Pathology, Oral Radiology . 2016;121(5):550–556. .5Queiroz P. M., Santaella G. M., da Paz T. D., Freitas D. Q. Evaluation of a metal artefact reduction tool on different positions of a metal object in the FOV. Dento Maxillo Facial Radiology . 2017;46(3, article 20160366) Montesinos G. A., de Castro Lopes S. L. P., Trivino T., et al. Subjective analysis of the application of enhancement filters on magnetic resonance imaging of the temporomandibular joint. Oral Surgery, Oral Medicine, Oral Pathology, Oral Radiology . 2019;127(6):552–559. doi: 10.1016/j.oooo.2018.11.015
17. Gregoris Rabelo L. E., Bueno M. D. R., Costa M., et al. Blooming artifact reduction using different cone-beam computed tomography software to analyze endodontically treated teeth with intracanal posts. Computers in Biology and Medicine . 2021;136, article 104679 doi: 10.1016/j.compbiomed.2021.104679
18. Estrela C., Costa M. V. C., Bueno M. R., et al. Potential of a new cone-beam CT software for blooming artifact reduction. Brazilian Dental Journal . 2020;31(6):582–588. doi: 10.1590/0103-6440202005899
19. Fontenele R. C., Farias Gomes A., Rosado L. P. L., Neves F. S., Freitas D. Q. Mapping the expression of beam hardening artefacts produced by metal posts positioned in different regions of the dental arch. Clinical Oral Investigations . 2021;25(2):571–579.
20. Mumford, D., and Shah, J. “Optimal approximation by piecewise smooth functions and associated variational problems,” Commun. Pure Appl. Math, vol. 42, pp. 577–685, 1989.
21. Li, C., Xu, C., Gui, C., and Fox, M. D. (2005). “Level set evolution without re-initialization: A new variational formulation,” in Proc. IEEE Conf. Computer Vision and Pattern Recognition, vol. 1, pp. 430–436.